Axionlike dark matter from the type-II seesaw mechanism

Wei Chao,[1,*] Mingjie Jin,[1,†] Hai-Jun Li,[2,1,‡] Ying-Quan Peng,[1,§] and Yue Wang[1,‖]

[1]*Center for Advanced Quantum Studies, Department of Physics, Beijing Normal University, Beijing 100875, China*

[2]*Key Laboratory of Theoretical Physics, Institute of Theoretical Physics, Chinese Academy of Sciences, Beijing 100190, China*

(Received 2 November 2022; revised 6 September 2023; accepted 21 May 2024; published 24 June 2024)

Although axionlike particles (ALPs) are popular dark matter candidates, their mass generation mechanisms as well as cosmic thermal evolutions are unclear. In this paper, we propose a new mass generation mechanism of an ALP during the electroweak phase transition in the presence of the type-II seesaw mechanism. In this scenario, the ALP gets mass uniquely at the electroweak scale, so there is a cutoff scale on the ALP oscillation temperature that is irrelevant to the specific mass of the ALP, serving as a distinctive feature of this scenario. Interactions of the ALP have been systematically studied, which shows that the ALP does not couple to diphotons. Instead, it couples to active neutrinos as well as the electron. Therefore, it can be boosted by cosmic rays and can be tested in proposed direct detection experiments with various condensed matter materials as targets.

DOI: 10.1103/PhysRevD.109.115027

I. INTRODUCTION

Various cosmological observations have confirmed the existence of cold dark matter (DM), which accounts for about 26.8% [1] of the cosmic energy budget. However, the particle nature of DM still eludes us. Axions [2–5] are one of the most popular DM candidates motivated by addressing the strong *CP* problem, with its mass induced by the QCD instanton and its relic abundance arising from the misalignment mechanism [6–11], which drives the coherent oscillation of the axion field around the minimum of the effective potential. Couplings of the axion to the standard model (SM) particles are model dependent and there are three general types of QCD axion models, Peccei-Quinn-Weinberg-Wilczek (PQWW) [2,3], Kim-Shifman-Vainshtein-Zakharov [12,13], and Dine-Fischler-Srednicki-Zhitnitsky [14,15] models, of which the PQWW axion is already excluded by the beam-dump experiments [16–18] and other axion models can be detected via their couplings to diphotons or SM fermions.

To relax property constraints to the QCD axions, more general classes of axionlike particle (ALP) DM models [19–35] were proposed, with the mass ranging from 10^{-22} eV to $\mathcal{O}(1)$ GeV [9,31], where the lower bound is from the fuzzy DM [36] and the upper bound is from the LHC limits. The mass generation mechanism as well as the relic abundance of axionlike DM are blurred and indistinct since scientists usually pay more attention to signals of ALPs in various experiments via detecting its coupling to photons [37–48] or SM fermions. However, it should be mentioned that the mass generation mechanism of the ALP is highly correlated with its interactions with the SM particles. So one cannot simply ignore these facts and directly apply the strategy of searching for QCD axions to the detection of the ALP. This issue has been concerned recently and several novel approaches have been proposed to address the relic abundance of the light scalar DM, such as the kinetic misalignment mechanism and the thermal misalignment mechanism [49,50], which supposes a feeble coupling between the DM and thermal fermions. These attempts provide novel insights to the origin of ALPs in the early Universe.

In this paper, we propose a new mechanism of generating the ALP mass during the electroweak phase transition with the help of a Higgs triplet Δ, which is the seesaw particle in the type-II seesaw mechanism [51–56]. Active neutrinos get Majorana mass as Δ develops a tiny but nonzero vacuum expectation value (VEV). We explicitly show that an ALP, which is the Goldstone boson arising from the spontaneous breaking of the global $U(1)_L$ symmetry and is usually called a Majoron, can get tiny mass through the

*chaowei@bnu.edu.cn
†jinmj507@gmail.com
‡lihaijun@itp.ac.cn
§yqpenghep@mail.bnu.edu.cn
‖wang_yue_222@163.com

quartic coupling with the Higgs triplet and the SM Higgs doublet Φ whenever the global lepton number is explicitly broken by the term $\mu\Phi^T i\sigma_2\Delta^\dagger\Phi + \text{H.c.}$ In such a scenario, symmetries break sequentially: the $U(1)_L$ first breaks at a high energy scale resulting in a massless ALP serving as dark energy, then electroweak symmetry is spontaneously broken leading to the mass generation of the ALP and active neutrinos. Once the mass becomes comparable to the Hubble parameter, the ALP begins to oscillate. We derive the relic density of the ALP by investing its thermal evolution and solving its equation of motion (EOM) analytically. To further investigate its signal, we explicitly derive couplings between the ALP and all the SM particles. Although there is no $aF_{\mu\nu}\tilde{F}^{\mu\nu}$ interaction, we expect that the ALP-electron interaction can be probed by the absorption of ALP DM in proposed direct detection experiments with condensed matter materials as targets.

II. FRAMEWORK

We assume that the $U(1)_L$ is spontaneously broken at high temperature by a Higgs mechanism when S, which is a complex scalar singlet carrying two units of the lepton number, gets a VEV. Additionally, the type-II seesaw mechanism is required for the origin of active neutrino masses, and S couples to the Higgs triplet Δ and the SM Higgs doublet Φ via the quartic interaction. The most general scalar potential is

$$\begin{aligned} V(S,\Phi,\Delta) = {} & V(\Phi,\Delta) - \mu_S^2(S^\dagger S) + \lambda_6(S^\dagger S)^2 \\ & + \lambda_7(S^\dagger S)(\Phi^\dagger\Phi) + \lambda_8(S^\dagger S)\mathrm{Tr}(\Delta^\dagger\Delta) \\ & + \mu\Phi^T i\sigma_2\Delta^\dagger\Phi + \lambda S\Phi^T i\sigma_2\Delta^\dagger\Phi + \text{H.c.}, \end{aligned} \tag{1}$$

where $V(\Phi,\Delta)$ is the most general potential for the type-II seesaw mechanism given in the section 1 of the Supplemental Material [57]. The quartic couplings $\lambda_{7,8}$ are relevant for the thermal mass of S. It is obvious that S may get nonzero VEV in the early Universe by assuming small quartic couplings, which is consistent with experimental observations [58–61], leaving the CP-odd component of S as the ALP. This ALP is massless at the early time until the temperature drops down to the electroweak scale. After the electroweak symmetry breaking (EWSB), when both Φ and Δ get nonzero VEVs, the ALP acquires a tiny mass double suppressed by the VEV of the Higgs triplet and the tiny parameter μ, which should be naturally small according to the naturalness principle of ‘t Hooft [62].

To analytically derive the mass of the ALP, the Φ, Δ, and S can be parametrized as

$$\Phi = \begin{bmatrix} \phi^+ \\ \frac{v_\phi+\phi+i\chi}{\sqrt{2}} \end{bmatrix}, \quad \Delta = \begin{bmatrix} \frac{\Delta^+}{\sqrt{2}} & \Delta^{++} \\ \Delta^0 & -\frac{\Delta^+}{\sqrt{2}} \end{bmatrix}, \quad S = \frac{v_s+\tilde{s}+i\tilde{a}}{\sqrt{2}}, \tag{2}$$

where $\Delta^0 = (v_\Delta + \delta + i\xi)/\sqrt{2}$ is the neutral component of the Higgs triplet, and v_ϕ, v_Δ, and v_s are the VEVs of Φ, Δ, and S, respectively. After the electroweak symmetry breaking, the remaining physical scalars are as follows: two charged scalar pairs $H^{\pm\pm}$ and $H^\pm$, two CP-odd scalars A and a, and three CP-even scalars h, H, and s, whose masses may be obtained by the diagonalization of their squared mass matrices. The detailed procedures of diagonalizations of all the scalar mass matrices are given in the Supplemental Material [57]. Then the ALP mass in the CP-odd sector can be written as

$$m_a^2 \simeq \frac{\sqrt{2}\mu v_\phi^2 v_\Delta(v_\phi^2 + 4v_\Delta^2)}{2v_\phi^2(v_\Delta^2 + v_s^2) + 8v_\Delta^2 v_s^2}. \tag{3}$$

In the limits $v_\Delta^2/v_\phi^2 \ll 1$ and $v_\Delta^2/v_s^2 \ll 1$, one has $m_a^2 \simeq \mu v_\phi^2 v_\Delta/(\sqrt{2}v_s^2)$, which is double suppressed by the parameters v_Δ and μ in the type-II seesaw mechanism and is thus naturally small.

Alternatively, the ALP mass can be derived from the ALP potential, whose expression can be obtained from the following phase transformations: $S \to e^{i\frac{a}{v_s}}S$, $\Delta \to e^{i\frac{a}{v_s}}\Delta$, $\Phi \to \Phi$, $\ell_L \to e^{i\frac{a}{2v_s}}\ell_L$, and $E_R \to e^{i\frac{a}{2v_s}}E_R$, where ℓ_L and E_R are the left-handed lepton doublets and right-handed lepton singlets, respectively. Then the only term relevant to the ALP potential is $e^{i\frac{a}{v_s}}\mu\Phi^T i\sigma_2\Delta^+\Phi + \text{H.c.}$ After EWSB, this term results in a cosinelike potential for the ALP,

$$\mu e^{-i\frac{a}{v_s}}\Phi^T i\sigma_2\Delta^\dagger\Phi + \text{H.c.} \supset \mu\frac{v_\phi^2 v_\Delta}{\sqrt{2}}\cos\left(\frac{a}{v_s}\right) + \cdots, \tag{4}$$

which involves a shift symmetry $a \to a + 2\pi N v_s$ (N is an integer), similar to the QCD axion case. In the limit of $a/v_s \ll 1$, one has $\cos(a/v_s) \simeq 1 - a^2/2v_s^2$, and the ALP mass can be written as $m_a^2 \simeq \mu v_\phi^2 v_\Delta/(\sqrt{2}v_s^2)$, which is consistent with the approximate expression in Eq. (3) derived by diagonalizing the squared mass matrix.

III. ALP DM

As discussed above, the ALP gets a tiny but nonzero mass via the type-II seesaw mechanism during the electroweak phase transition at the critical temperature $T_C \simeq 160$ GeV [63]. The radiation corrections from both one- and two-loop diagrams are suppressed by the tiny factor of μ^2. Neglecting the radiative corrections, the temperature-dependent ALP mass can be written as

$$m_a^2(T) = \begin{cases} \frac{\mu v_\phi^2(T) v_\Delta(T)}{\sqrt{2}f_a^2}, & T \le T_C \\ 0, & T > T_C \end{cases} \tag{5}$$

where $f_a = v_s$, $v_\phi(T)$ and $v_\Delta(T)$ are the temperature-dependent VEVs of the SM Higgs and Higgs triplet, respectively. The EOM of the homogeneous ALP field a ($a \equiv \theta f_a$) in the Friedmann-Robertson-Walker universe can be written as [6–8]

$$\ddot{\theta} + 3H(T)\dot{\theta} + m_a^2(T)\theta = 0, \tag{6}$$

where the dot denotes the derivative with respect to time, and $H(T) \equiv \dot{R}/R$ is the Hubble parameter in terms of the scale factor R. In the radiation-dominated epoch, we have $H(T) = 1/(2t) = 1.66\sqrt{g_*(T)}T^2/m_{\rm pl}$, where g_* is the effective number of the degrees of freedom, and $m_{\rm pl} = 1.221 \times 10^{19}$ GeV is the Planck mass. The initial conditions are taken as $\theta(t_i) = \sqrt{\langle\theta_{a,i}^2\rangle}$ and $\dot{\theta}(t_i) = 0$, where the angle brackets denote the initial misalignment angle $\theta(t_i)$ averaged over $[-\pi, \pi)$ [10]. The value of $\langle\theta_{a,i}^2\rangle$ depends on whether the $U(1)_L$ breaking occurs before the inflation ends or after the inflation [10,30].

In general, the ALP becomes dynamical and starts to oscillate when $m_a(T_{\rm osc}) = 3H(T_{\rm osc})$ [9–11], where $T_{\rm osc}$ is the oscillation temperature. Before the EWSB, the ALP is massless and the angle θ remains a constant with the initial value $\theta(t) = \theta(t_i)$. Therefore, there is an upper bound on the oscillation temperature $T_{\rm osc}^{\rm max} \equiv T_{\rm C}$, which leads to the existence of a critical mass

$$m_{a\rm C} = 1.079 \times 10^{-4}\ \text{eV}. \tag{7}$$

The oscillation temperature can be divided into two cases

$$T_{\rm osc} = \begin{cases} T_*, & m_a < m_{a\rm C} \\ T_{\rm C}, & m_a \geq m_{a\rm C} \end{cases} \tag{8}$$

where T_* is derived from the condition $m_a = 3H(T_*)$. Equation (8) implies that the traditional oscillation condition is only available to the case $m_a < m_{a\rm C}$. For $m_a \geq m_{a\rm C}$, the oscillation temperature is always equal to the critical temperature $T_{\rm C}$, as shown in Fig. 1. Note that we use the parameter $3H$ instead of the Hubble parameter H to better show the critical point given by Eq. (8).

We now investigate the evolution of the ALP, which is frozen at the initial value by the Hubble friction at early times ($3H > m_a$) and behaves as dark energy. As the temperature T of the Universe drops to $T_{\rm osc}$ given by Eq. (8), the ALP starts to oscillate with damped amplitude, and its energy density scales as R^{-3}, which is similar to the ordinary matter [9,10], until the angle θ oscillates around the potential minimum of the ALP at the late time. The evolution of θ can be described by the *analytical* solution of EOM in the radiation-dominated universe when $H > H_E \sim 10^{-28}$ eV [9,64], where H_E is the Hubble rate at the matter-radiation equality in ΛCDM. The exact analytical expression is given in Sec. B of the Supplemental

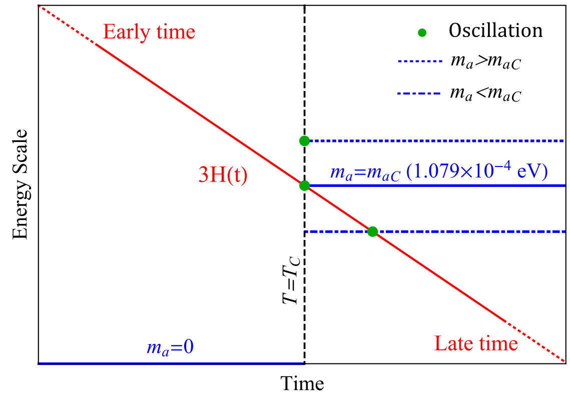

FIG. 1. The evolution of the energy scales for ALP mass m_a (blue line) and the Hubble parameter (red line) as a function of the time. Three cases of m_a are shown for comparisons. The green intersections represent the temperatures when the oscillation begins. The vertical dashed line represents the critical temperature ($T_{\rm C}$).

Material [57]. Alternatively, we can also *numerically* solve Eq. (6) with the given initial values. Here we consider the postinflationary scenario and take the initial value as $\theta(t_i) = \pi/\sqrt{3}$ [10,30]. The analytical and numerical results are shown in Fig. 2 with the two benchmark ALP masses. We find that the numerical results of the evolution are consistent with the analytical ones.

The energy density of the ALP is $\rho_a(t) = \dot{\theta}^2(t)f_a^2/2 + m_a^2(T)\theta^2(t)f_a^2/2$. Since the ratio of ALP number density to the entropy density is conserved, the ALP energy density at the present can be written as $\rho_a(T_0) \simeq \rho_a(R_{\rm osc})(R_{\rm osc}/R)^3 = 1/2 m_a(T_{\rm osc})m_a(T_0)f_a^2\langle\theta_{a,i}^2\rangle s(T_0)/s(T_{\rm osc})$ [9–11], where T_0 is the cosmic microwave background temperature at present, and $s = 2\pi^2 g_{*s}T^3/45$ is the entropy density with

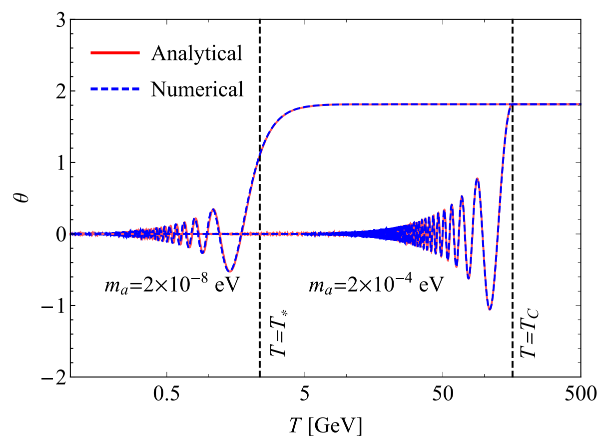

FIG. 2. The analytical (solid red) and numerical (dashed blue) evolution of θ as a function of T for two benchmark ALP masses $m_a < m_{a\rm C}$ ($m_a = 2\times10^{-8}$ eV) and $m_a > m_{a\rm C}$ ($m_a = 2\times10^{-4}$ eV). The vertical dashed lines correspond to the oscillation temperatures.

g_{*s} as the relativistic degrees of freedom of the entropy. The ALP mass is almost temperature independent, which indicates $m_a(T_{\rm osc}) = m_a(T_0) = m_a$, so the ALP energy density at present is

$$\rho_a(T_0) \simeq \frac{1}{2} m_a^2 f_a^2 \langle \theta_{a,i}^2 \rangle \frac{g_{*s}(T_0)}{g_{*s}(T_{\rm osc})} \left(\frac{T_0}{T_{\rm osc}}\right)^3. \tag{9}$$

The relic density of ALP at present is defined as $\Omega_a h^2 = (\rho_a(T_0)/\rho_{c,0})h^2$ [9,10], where $\rho_{c,0} \equiv 3m_{\rm pl}^2 H_0^2/(8\pi)$ is the critical energy density, $T_0 = 2.4 \times 10^{-4}$ eV, and $g_{*s}(T_0) = 3.94$ [65]. Combining these parameters with Eq. (9), the relic density of ALP can be estimated as

$$\Omega_a h^2 = \begin{cases} 0.056\langle \theta_{a,i}^2 \rangle \left(\frac{3.94}{g_{*s}(T_*)}\right) \left(\frac{g_*(T_*)}{3.36}\right)^{\frac{3}{4}} \\ \times \left(\frac{f_a}{10^{13}\ \mathrm{GeV}}\right)^2 \left(\frac{m_a}{10^{-7}\ \mathrm{eV}}\right)^{\frac{1}{2}}, m_a < m_{a\mathrm{C}}, \\ 0.0078\langle \theta_{a,i}^2 \rangle \left(\frac{f_a}{10^{10}\ \mathrm{GeV}}\right)^2 \left(\frac{m_a}{10^{-2}\ \mathrm{eV}}\right)^2, \\ m_a \geq m_{a\mathrm{C}}. \end{cases} \tag{10}$$

Since the initial misalignment angle $\langle \theta_{a,i}^2 \rangle^{1/2} \sim \mathcal{O}(1)$, the relic density is almost determined by the decay constant f_a and its mass m_a. In Fig. 3, we show the relic density $\Omega_a h^2$ as a function of m_a with the four benchmark values of $f_a \sim \mathcal{O}(10^{10}\text{–}10^{13})$ GeV. The vertical black dotted line represents the critical mass $m_{a\mathrm{C}}$, on two sides of which the ALP density evolves differently. We find that there exists the allowed parameter space that may address the observed DM relic abundance, $\Omega_a h^2 \simeq 0.12$ [1,65].

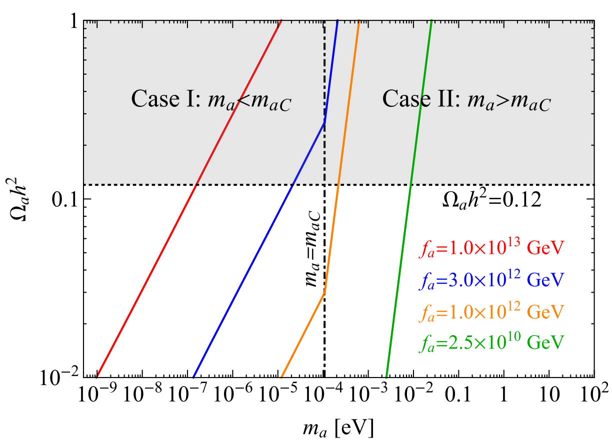

FIG. 3. The relic density $\Omega_a h^2$ as a function of m_a for various f_a. The vertical dotted line represents the critical mass ($m_{a\mathrm{C}}$). The initial misalignment angle is taken as $\theta(t_i) = \pi/\sqrt{3}$. The gray region is excluded by the overabundance of DM.

IV. ALP-SM INTERACTIONS

The ALP interacts with the SM particles via the scalar potential as well as the Yukawa interaction. In the following, we investigate the coupling between the ALP and ordinary matters, including the Higgs bosons, leptons, and electroweak gauge bosons, and show constraints on the parameter space of the model in the $m_a - f_a^{-1}$ plane from projected direct detection experiments. At first, the ALP couples to the SM Higgs in form $\lambda_{haa} haa$ with the coupling

$$\lambda_{haa}\colon\ -\lambda U_{11} V_{13} V_{23} f_a + \frac{1}{2} \lambda U_{21} V_{13}^2 f_a, \tag{11}$$

where U_{ij}, V_{ij} $(i, j = 1, 2, 3)$ are the orthogonal matrices diagonalizing squared scalar matrices given in the Supplemental Material [57]. Given that the SM Higgs decays into two ALPs ($h \to aa$), the constraint of Higgs invisible decay from the LHC set an upper bound on the coupling $\lambda_{haa} < 1.536$ GeV [66]. We have checked that the coupling predicted by this model keeps this constraint.

The interactions of the ALP with leptons and electroweak gauge bosons arise from the chiral anomaly. As mentioned above, both scalars and leptons undergo an ALP-dependent transformation of the fields as $S \to e^{i\frac{a}{f_a}} S$, $\Delta \to e^{i\frac{a}{f_a}} \Delta$, $\Phi \to \Phi$, $\ell_L \to e^{i\frac{a}{2f_a}} \ell_L$, and $E_R \to e^{i\frac{a}{2f_a}} E_R$. Given these transformations, the variation of the action results in couplings of the ALP to both leptons and electroweak gauge bosons due to the electroweak anomaly, which can be written as follows:

$$\begin{aligned} \delta\mathcal{L} = & \frac{m_\nu}{2f_a} a\bar{\nu} i\gamma^5 \nu - N_f \frac{\alpha_{\rm em}}{16\pi f_a \sin^2\theta_w} a W_{\mu\nu}^+ \tilde{W}^{-\mu\nu} \\ & - N_f \frac{\alpha_{\rm em}}{32\pi f_a \sin\theta_w \cos\theta_w} a (Z_{\mu\nu} \tilde{F}^{\mu\nu} + F_{\mu\nu} \tilde{Z}^{\mu\nu}) \\ & - N_f \frac{\alpha_{\rm em}}{8\pi f_a \sin^2\theta_w \cos^2\theta_w} \left(\frac{1}{2} - \sin^2\theta_w\right) a Z_{\mu\nu} \tilde{Z}^{\mu\nu}, \end{aligned} \tag{12}$$

where $N_f (= 3)$ is the generation of the lepton family, $\alpha_{\rm em}$ is the fine-structure constant, and θ_w is the weak mixing angle. It should be noted that the left- and right-handed charged leptons contribute oppositely to the anomaly, so the ALP interacts with electrons only through its mixing with the CP-odd component of the SM Higgs,

$$\mathcal{L}_{aee} \simeq 2 \frac{v_\Delta^2}{v_\phi^2} \frac{m_e}{f_a} a\bar{e} i\gamma^5 e. \tag{13}$$

The effective ALP-electron coupling is then $g_{aee} = 2v_\Delta^2 m_e/(v_\phi^2 f_a)$, which is suppressed with respect to the standard case due to the small v_Δ.

For the ALP-neutrino coupling, in addition to the first term in Eq. (12), the Yukawa interaction of the Higgs triplet with lepton doublets also induces the ALP-neutrino interaction via the mixing of CP-odd scalars, and one has

TABLE I. The comparison between the QCD axion and ALP.

	QCD axion	ALP
Shift symmetry	$a \to a + c$	
Chiral transformation	$q \to e^{i\gamma_5 \frac{a}{2f_a} Q_a} q$	$\ell_L \to e^{i\frac{a}{2f_a}} \ell_L$, $E_R \to e^{i\frac{a}{2f_a}} E_R$
Source of mass	Chiral anomaly (QCD instantons)	μ-term (EWSB)
Potential	$m_a^2 f_a^2 [1 - \cos(\frac{a}{f_a})]$	$\mu \frac{v_\phi^2 v_\Delta}{\sqrt{2}} \cos(\frac{a}{f_a})$
Periodic symmetry	$a \to a + 2\pi N f_a$	

$\mathcal{L}^Y_{a\nu\nu} = -i(V_{23} m_\nu / 2v_\Delta) a \overline{\nu_L^C} \nu_L + \mathrm{H.c.}$ In the limits $v_\Delta^2 / v_\phi^2 \ll 1$ and $v_\Delta^2 / f_a^2 \ll 1$, we have $V_{23} \simeq v_\Delta / f_a$ and thus the interaction of the ALP with active neutrinos can be written as

$$\mathcal{L}_{a\nu\nu} = \frac{m_\nu}{2f_a} a \bar{\nu} i\gamma^5 \nu + \mathcal{L}^Y_{a\nu\nu} \approx \frac{m_\nu}{f_a} a \bar{\nu} i\gamma^5 \nu. \tag{14}$$

Obviously, the above interaction may cause the matter effect in neutrino oscillations. As an illustration, we discuss the neutrino oscillation probability in a dense axion environment. In the meanwhile, we show that the W-mass anomaly observed by the CDF Collaboration can also be explained by the TeV-scale type-II seesaw. The detailed discussions are quoted in the Supplemental Material [57].

We list the correlation between the QCD axion and the ALP in this model in Table I. As can be seen, the ALP is very similar to the QCD axion except for the mass generation mechanism, which is the most remarkable feature of these kinds of ALPs.

Now we investigate the signal of the ALP in terrestrial experiments. Considering that there is no $aF\tilde{F}$ interaction, the traditional cavity observation experiment cannot be applied here. Instead, we can study the signal of the ALP in projected direct detection experiments with various condensed matter materials as the target, considering that the kinetic energy of the axion is small. References [67,68] have discussed the absorption of pseudoscalar DM in semiconductors and superconductors, revealing competitive constraints on the g_{aee} coupling for DM masses ranging from meV to keV with respect to the astrophysical bounds. In Fig. 4, we show projected constraints on the parameter space of the ALP in the $m_a - f_a^{-1}$ plane by assuming no observation of the absorptions of the ALP in superconducting aluminum, germanium, and silicon semiconducting targets with a 1 kg/yr (solid lines) and 1 ton/yr (dashed lines) exposures, respectively. Astrophysical constraints, including the measurements of all-flavor solar neutrino flux [69], XENONnT (based on solar axion signal [70] and axioelectric processes [71]), and the axions emitted by red giants [72], are also presented.

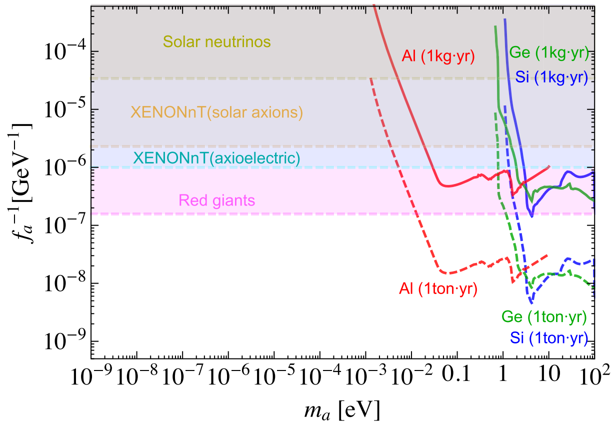

FIG. 4. Constraints in the $m_a - f_a^{-1}$ plane for $v_\Delta = 7$ GeV. The red, green, and blue solid (dashed) curves represent projected constraints arising from the absorptions of ALPs by Al, Ge, and Si with a 1 kg/yr (1 t/yr) exposure [67,68]. Other limits are taken from the solar neutrinos [69], XENONnT (solar axion [70] and axioelectric [71]), and red giants [72].

V. SUMMARY

In this paper, we have proposed a new mass generation mechanism of ALPs with the help of the type-II seesaw mechanism that gives rise to the active neutrino Majorana masses. The typical oscillation temperature of the ALP shows a cutoff at the critical temperature of the EWSB, which is the typical trapping of this kind of ALP. Because of the ALP-electron interactions, it might be detected through the axioelectric processes of the ALP in XENONnT and PandaX4T and through the absorption of the ALP in projected direct detection experiments with various semiconducting and superconducting materials as targets. All these observations open up a new perspective for exploring the origin of the ALP mass and detecting the signal of the ALP with new approaches.

ACKNOWLEDGMENTS

The authors would like to thank Sara Khatibi for helpful discussions. This work was supported by the National Natural Science Foundation of China (NSFC) (Grants No. 11775025 and No. 12175027).

[1] N. Aghanim *et al.* (Planck Collaboration), Planck 2018 results. VI. Cosmological parameters, Astron. Astrophys. **641**, A6 (2020); **652**, C4(E) (2021).
[2] R. D. Peccei and Helen R. Quinn, Constraints imposed by *CP* conservation in the presence of instantons, Phys. Rev. D **16**, 1791 (1977).
[3] R. D. Peccei and Helen R. Quinn, *CP* conservation in the presence of instantons, Phys. Rev. Lett. **38**, 1440 (1977).
[4] Steven Weinberg, A new light boson?, Phys. Rev. Lett. **40**, 223 (1978).
[5] Frank Wilczek, Problem of strong *P* and *T* invariance in the presence of instantons, Phys. Rev. Lett. **40**, 279 (1978).
[6] Michael Dine and Willy Fischler, The not so harmless axion, Phys. Lett. **120B**, 137 (1983).
[7] John Preskill, Mark B. Wise, and Frank Wilczek, Cosmology of the invisible axion, Phys. Lett. **120B**, 127 (1983).
[8] L. F. Abbott and P. Sikivie, A cosmological bound on the invisible axion, Phys. Lett. **120B**, 133 (1983).
[9] David J. E. Marsh, Axion cosmology, Phys. Rep. **643**, 1 (2016).
[10] Luca Di Luzio, Maurizio Giannotti, Enrico Nardi, and Luca Visinelli, The landscape of QCD axion models, Phys. Rep. **870**, 1 (2020).
[11] Raymond T. Co, Lawrence J. Hall, and Keisuke Harigaya, Axion kinetic misalignment mechanism, Phys. Rev. Lett. **124**, 251802 (2020).
[12] Jihn E. Kim, Weak interaction singlet and strong *CP* invariance, Phys. Rev. Lett. **43**, 103 (1979).
[13] Mikhail A. Shifman, A. I. Vainshtein, and Valentin I. Zakharov, Can confinement ensure natural *CP* invariance of strong interactions?, Nucl. Phys. **B166**, 493 (1980).
[14] Michael Dine, Willy Fischler, and Mark Srednicki, A simple solution to the strong *CP* problem with a harmless axion, Phys. Lett. **104B**, 199 (1981).
[15] A. R. Zhitnitsky, On possible suppression of the axion hadron interactions (in Russian), Sov. J. Nucl. Phys. **31**, 260 (1980).
[16] Jihn E. Kim, Light pseudoscalars, particle physics and cosmology, Phys. Rep. **150**, 1 (1987).
[17] H. Faissner, E. Frenzel, W. Heinrigs, A. Preussger, D. Samm, and U. Samm, Limit on axion decay into an electron pair, Phys. Lett. **96B**, 201 (1980).
[18] H. Faissner, E. Frenzel, W. Heinrigs, A. Preussger, D. Samm, and U. Samm, Observation of the two-photon decay of a light penetrating particle, Phys. Lett. **103B**, 234 (1981).
[19] Y. Chikashige, Rabindra N. Mohapatra, and R. D. Peccei, Are there real Goldstone bosons associated with broken lepton number?, Phys. Lett. **98B**, 265 (1981).
[20] G. B. Gelmini and M. Roncadelli, Left-handed neutrino mass scale and spontaneously broken lepton number, Phys. Lett. **99B**, 411 (1981).
[21] Frank Wilczek, Axions and family symmetry breaking, Phys. Rev. Lett. **49**, 1549 (1982).
[22] Z. G. Berezhiani and M. Yu. Khlopov, The theory of broken gauge symmetry of families. (In Russian), Sov. J. Nucl. Phys. **51**, 739 (1990).
[23] Joerg Jaeckel, A family of WISPy dark matter candidates, Phys. Lett. B **732**, 1 (2014).
[24] Edward Witten, Some properties of O(32) superstrings, Phys. Lett. **149B**, 351 (1984).
[25] Joseph P. Conlon, The QCD axion and moduli stabilisation, J. High Energy Phys. 05 (2006) 078.
[26] Michele Cicoli, Mark Goodsell, and Andreas Ringwald, The type IIB string axiverse and its low-energy phenomenology, J. High Energy Phys. 10 (2012) 146.
[27] Howard M. Georgi, Lawrence J. Hall, and Mark B. Wise, Grand unified models with an automatic Peccei-Quinn symmetry, Nucl. Phys. **B192**, 409 (1981).
[28] A. G. Dias, A. C. B. Machado, C. C. Nishi, A. Ringwald, and P. Vaudrevange, The quest for an intermediate-scale accidental axion and further ALPs, J. High Energy Phys. 06 (2014) 037.
[29] Kang-Sin Choi, Hans Peter Nilles, Saul Ramos-Sanchez, and Patrick K. S. Vaudrevange, Accions, Phys. Lett. B **675**, 381 (2009).
[30] A. Ringwald, Axions and axion-like particles, in 49th Rencontres de Moriond on Electroweak Interactions and Unified Theories (2014), pp. 223–230, arXiv:1407.0546.
[31] Martin Bauer, Mathias Heiles, Matthias Neubert, and Andrea Thamm, Axion-like particles at future colliders, Eur. Phys. J. C **79**, 74 (2019).
[32] Matías M. Reynoso, Oscar A. Sampayo, and Agustín M. Carulli, Neutrino interactions with ultralight axion-like dark matter, Eur. Phys. J. C **82**, 274 (2022).
[33] Aharon Davidson and Kameshwar C. Wali, Minimal flavor unification via multigenerational Peccei-Quinn symmetry, Phys. Rev. Lett. **48**, 11 (1982).
[34] Aharon Davidson, V. P. Nair, and Kameshwar C. Wali, Peccei-Quinn symmetry as flavor symmetry and grand unification, Phys. Rev. D **29**, 1504 (1984).
[35] Aharon Davidson, V. P. Nair, and Kameshwar C. Wali, Mixing angles and *CP* violation in the SO(10) X U(1)-(pq) model, Phys. Rev. D **29**, 1513 (1984).
[36] Wayne Hu, Rennan Barkana, and Andrei Gruzinov, Cold and fuzzy dark matter, Phys. Rev. Lett. **85**, 1158 (2000).
[37] P. Sikivie, Experimental tests of the invisible axion, Phys. Rev. Lett. **51**, 1415 (1983); **52**, 695(E) (1984).
[38] Georg Raffelt and Leo Stodolsky, Mixing of the photon with low mass particles, Phys. Rev. D **37**, 1237 (1988).
[39] S. Andriamonje *et al.* (CAST Collaboration), An improved limit on the axion-photon coupling from the CAST experiment, J. Cosmol. Astropart. Phys. 04 (2007) 010.
[40] Klaus Ehret *et al.*, New ALPS results on hidden-sector lightweights, Phys. Lett. B **689**, 149 (2010).
[41] A. Abramowski *et al.* (H.E.S.S. Collaboration), Constraints on axionlike particles with H.E.S.S. from the irregularity of the PKS 2155-304 energy spectrum, Phys. Rev. D **88**, 102003 (2013).
[42] M. Ajello *et al.* (Fermi-LAT Collaboration), Search for spectral irregularities due to photon–axionlike-particle oscillations with the Fermi Large Area Telescope, Phys. Rev. Lett. **116**, 161101 (2016).
[43] V. Anastassopoulos *et al.* (CAST Collaboration), New CAST limit on the axion-photon interaction, Nat. Phys. **13**, 584 (2017).
[44] Alexander V. Gramolin, Deniz Aybas, Dorian Johnson, Janos Adam, and Alexander O. Sushkov, Search for axion-like dark matter with ferromagnets, Nat. Phys. **17**, 79 (2021).
[45] Hai-Jun Li, Jun-Guang Guo, Xiao-Jun Bi, Su-Jie Lin, and Peng-Fei Yin, Limits on axion-like particles from Mrk 421

with 4.5-year period observations by ARGO-YBJ and Fermi-LAT, Phys. Rev. D **103**, 083003 (2021).
[46] Chiara P. Salemi *et al.*, Search for low-mass axion dark matter with ABRACADABRA-10 cm, Phys. Rev. Lett. **127**, 081801 (2021).
[47] Júlia Sisk Reynés, James H. Matthews, Christopher S. Reynolds, Helen R. Russell, Robyn N. Smith, and M. C. David Marsh, New constraints on light axion-like particles using Chandra transmission grating spectroscopy of the powerful cluster-hosted quasar H1821 + 643, Mon. Not. R. Astron. Soc. **510**, 1264 (2021).
[48] Hai-Jun Li, Probing photon-ALP oscillations from the flat spectrum radio quasar 4C + 21.35, Phys. Lett. B **829**, 137047 (2022).
[49] Brian Batell and Akshay Ghalsasi, Thermal misalignment of scalar dark matter, Phys. Rev. D **107**, L091701 (2023).
[50] Eung Jin Chun, Bosonic dark matter in a coherent state driven by thermal fermions, Phys. Lett. B **825**, 136880 (2022).
[51] George Lazarides, Q. Shafi, and C. Wetterich, Proton lifetime and fermion masses in an SO(10) model, Nucl. Phys. **B181**, 287 (1981).
[52] Rabindra N. Mohapatra and Goran Senjanovic, Neutrino masses and mixings in gauge models with spontaneous parity violation, Phys. Rev. D **23**, 165 (1981).
[53] W. Konetschny and W. Kummer, Nonconservation of total lepton number with scalar bosons, Phys. Lett. **70B**, 433 (1977).
[54] T. P. Cheng and Ling-Fong Li, Neutrino masses, mixings and oscillations in $SU(2) \times U(1)$ models of electroweak interactions, Phys. Rev. D **22**, 2860 (1980).
[55] M. Magg and C. Wetterich, Neutrino mass problem and gauge hierarchy, Phys. Lett. **94B**, 61 (1980).
[56] J. Schechter and J. W. F. Valle, Neutrino masses in $SU(2) \times U(1)$ theories, Phys. Rev. D **22**, 2227 (1980).
[57] See Supplemental Material at http://link.aps.org/supplemental/10.1103/PhysRevD.109.115027 for detail.
[58] Robert M. Schabinger and James D. Wells, A minimal spontaneously broken hidden sector and its impact on Higgs boson physics at the large hadron collider, Phys. Rev. D **72**, 093007 (2005).
[59] Brian Patt and Frank Wilczek, Higgs-field portal into hidden sectors, arXiv:hep-ph/0605188.
[60] Giovanni Marco Pruna and Tania Robens, Higgs singlet extension parameter space in the light of the LHC discovery, Phys. Rev. D **88**, 115012 (2013).
[61] D. López-Val and T. Robens, Δr and the W-boson mass in the singlet extension of the standard model, Phys. Rev. D **90**, 114018 (2014).
[62] Gerard 't Hooft, Naturalness, chiral symmetry, and spontaneous chiral symmetry breaking, NATO Sci. Ser. B **59**, 135 (1980).
[63] Michela D'Onofrio, Kari Rummukainen, and Anders Tranberg, Sphaleron rate in the minimal standard model, Phys. Rev. Lett. **113**, 141602 (2014).
[64] Daniel Baumann, Inflation, in *Theoretical Advanced Study Institute in Elementary Particle Physics: Physics of the Large and the Small* (World Scientific, 2011), pp. 523–686.
[65] Martin Bauer and Tilman Plehn, *Yet Another Introduction to Dark Matter: The Particle Physics Approach*, Lecture Notes in Physics Vol. 959 (Springer, Cham, 2019).
[66] P. A. Zyla *et al.* (Particle Data Group), Review of particle physics, Prog. Theor. Exp. Phys. **2020**, 083C01 (2020).
[67] Yonit Hochberg, Tongyan Lin, and Kathryn M. Zurek, Absorption of light dark matter in semiconductors, Phys. Rev. D **95**, 023013 (2017).
[68] Yonit Hochberg, Tongyan Lin, and Kathryn M. Zurek, Detecting ultralight bosonic dark matter via absorption in superconductors, Phys. Rev. D **94**, 015019 (2016).
[69] Paolo Gondolo and Georg G. Raffelt, Solar neutrino limit on axions and keV-mass bosons, Phys. Rev. D **79**, 107301 (2009).
[70] E. Aprile *et al.* (XENON Collaboration), Search for new physics in electronic recoil data from XENONnT, Phys. Rev. Lett. **129**, 161805 (2022).
[71] Javier Redondo, Solar axion flux from the axion-electron coupling, J. Cosmol. Astropart. Phys. 12 (2013) 008.
[72] Francesco Capozzi and Georg Raffelt, Axion and neutrino bounds improved with new calibrations of the tip of the red-giant branch using geometric distance determinations, Phys. Rev. D **102**, 083007 (2020).